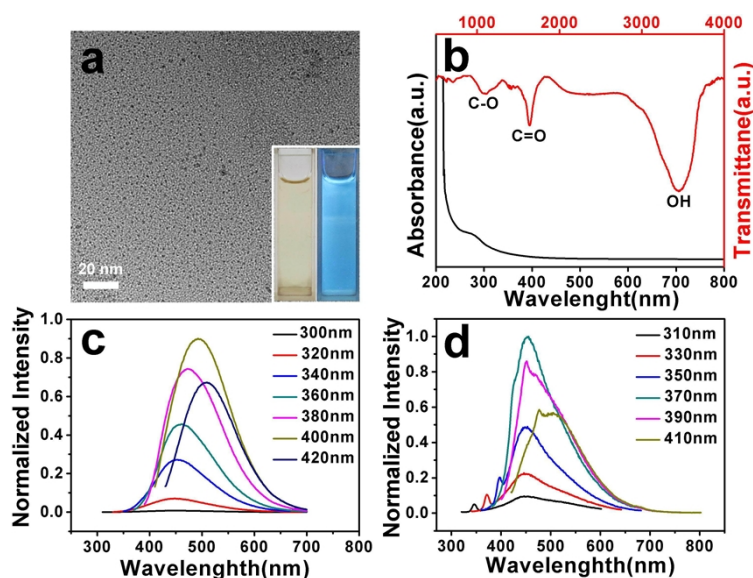
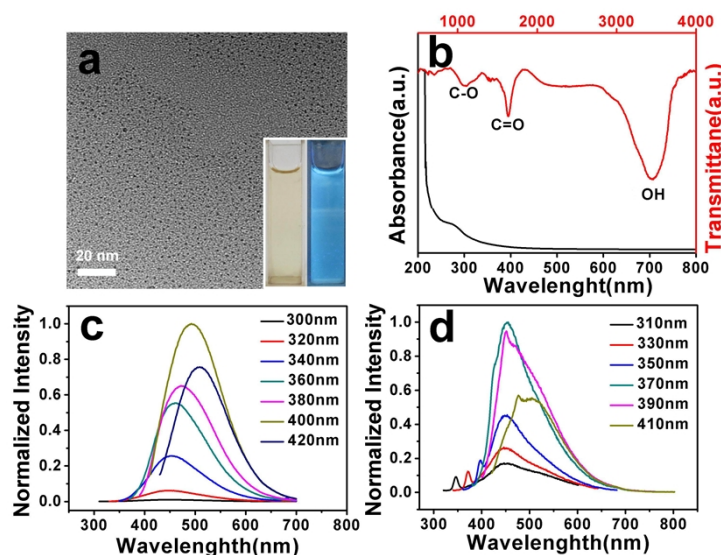


## Carbon dots from PEG for high sensitive detection of levodopa

### Supporting information



**Figure S1.** (a) Typical TEM image of CDs1, inset are the digital photos of CDs1 under visible and UVlight (at 365 nm excitation). (b) UV-vis absorption and FTIR spectra of CDs1 (black and red lines, respectively). (c and d) PL spectra of CDs1 with different excitation wavelengths in the water and PB (pH=6.8), respectively.



**Figure S2.** (a) Typical TEM image of CDs3, inset are the digital photos of CDs3 under visible and UVlight (at 365 nm excitation). (b) UV-vis absorption and FTIR spectra of CDs3 (black and red lines, respectively). (c and d) PL spectra of CDs3 with different excitation wavelengths in the water and PB (pH=6.8), respectively.

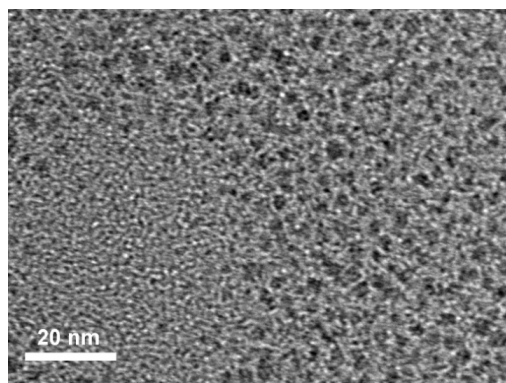


**Figure S3.** Typical TEM image of CDs4.

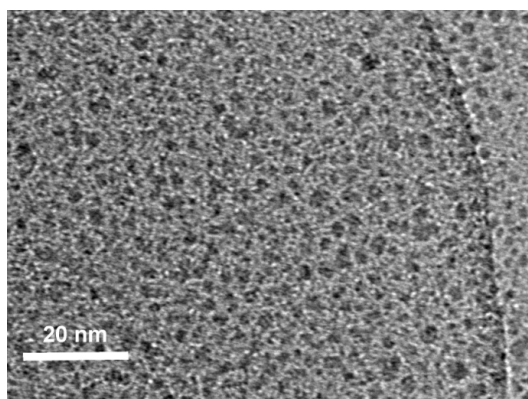


**Figure S4.** Typical TEM image of CDs5.

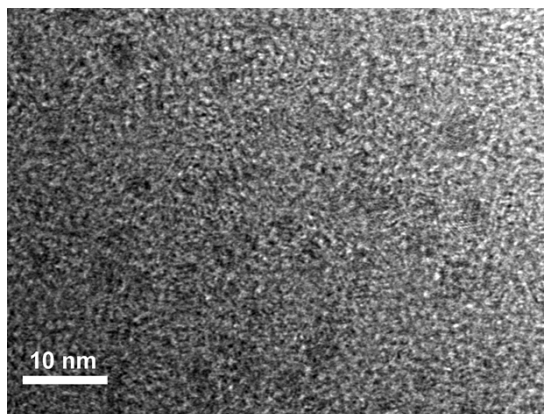


**Figure S5.** Typical TEM image of CDs6.

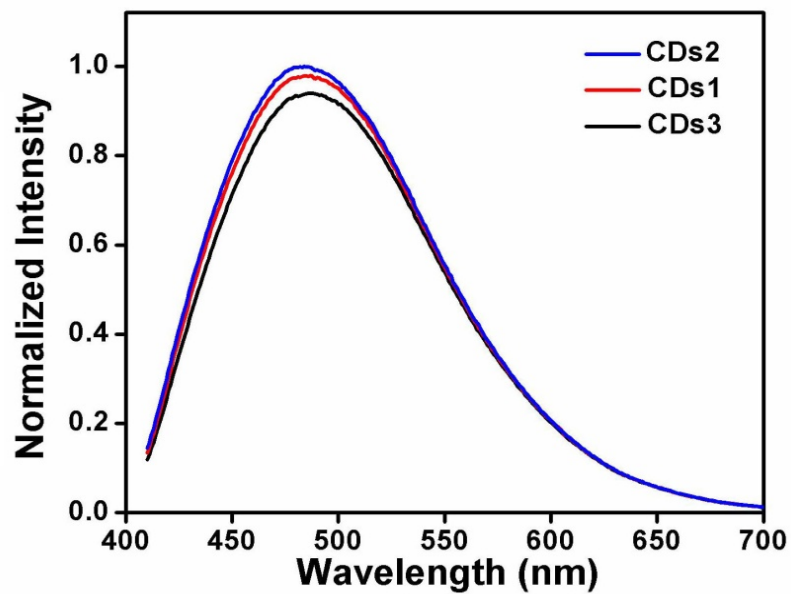


Figure S6. The PL spectra of different CDs fluorescence intensity.

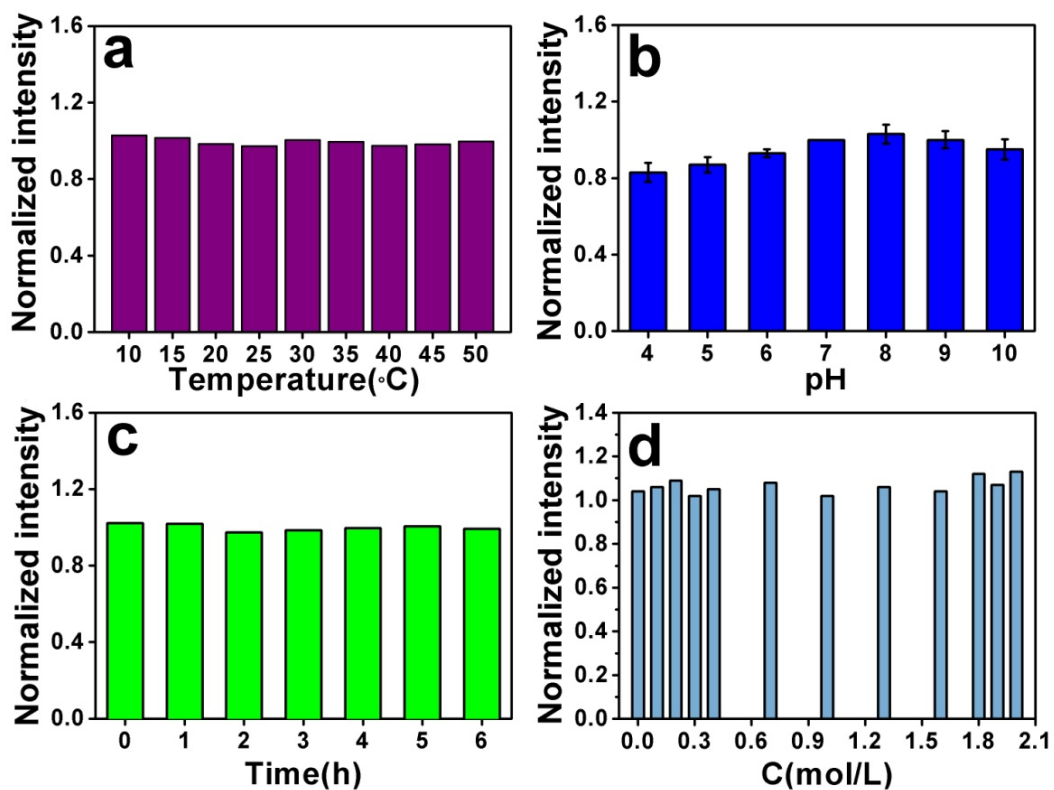
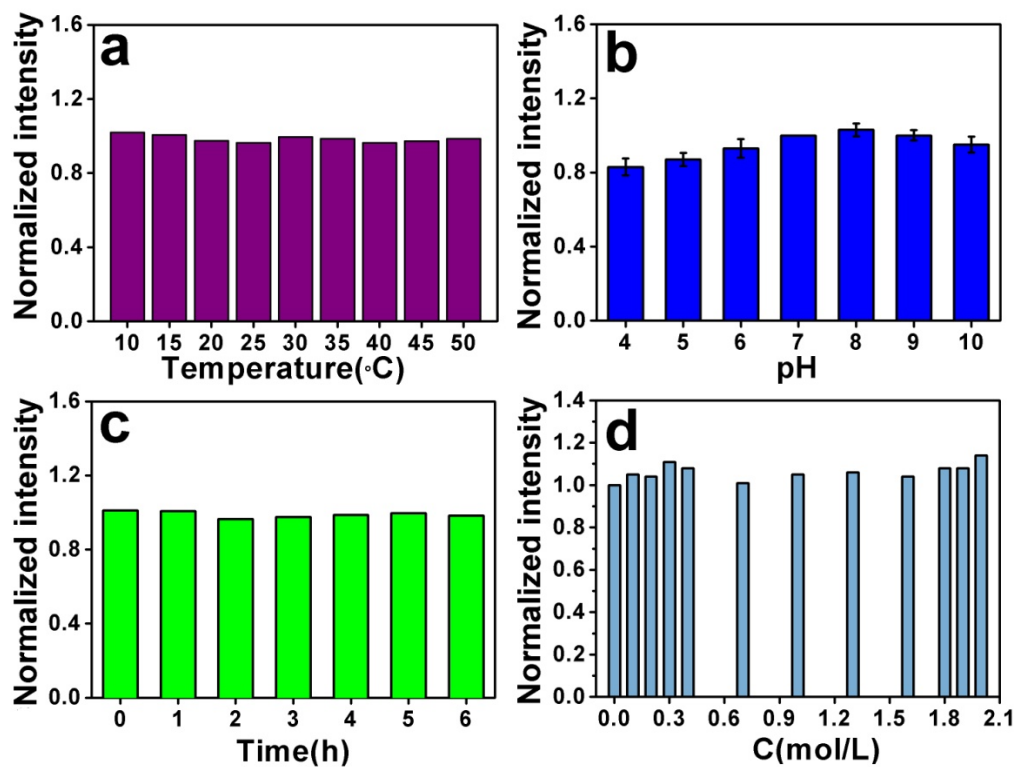
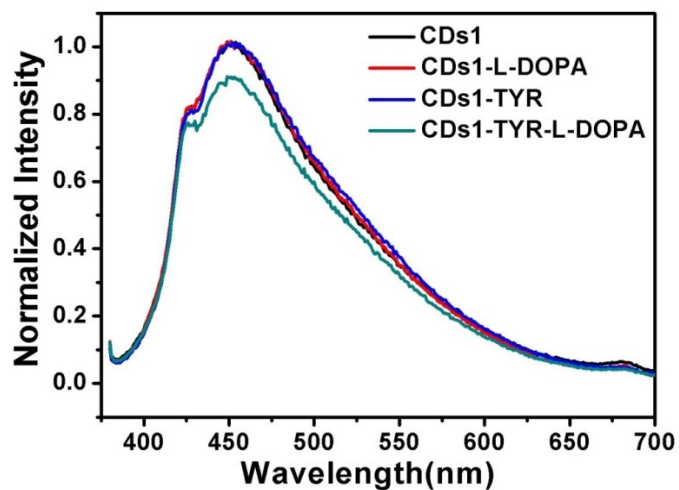


Figure S7. The effects of different temperatures(a), pH (b), stabilization time (c) and ionic strength in NaCl aqueous solution (d) on the normalized fluorescence intensity of CDs1 in PB solution.



**Figure S8.** The effects of different temperatures (a), pH (b), stabilization time (c) and ionic strength in NaCl aqueous solution (d) on the normalized fluorescence intensity of CDs3 in PB solution.



**Figure S9.** The fluorescence spectra of CDs1 (black line), CDs1 in the presence of 0.32 mM L-DOPA (CDs1-L-DOPA, red line), CDs1 in the presence of 20  $\mu\text{g mL}^{-1}$  TYR (CDs1-TYR, blue line), and CDs1 in the presence of a mixture containing 20  $\mu\text{g mL}^{-1}$  TYR and 0.32 mM L-DOPA (CDs1-TYR-L-DOPA, green line), respectively.

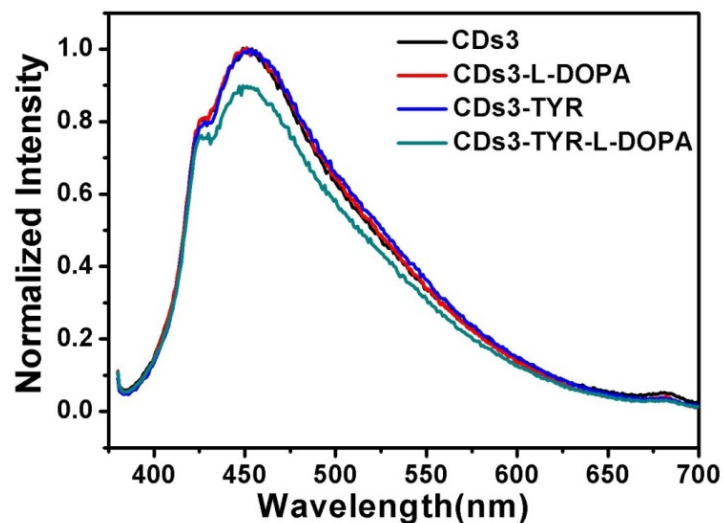


**Figure S10.** The fluorescence spectra of CDs3 (black line), CDs3 in the presence of 0.32 mM L-DOPA(CDs3-L-DOPA, red line), CDs3 in the presence of 20 $\mu\text{g mL}^{-1}$  TYR (CDs3-TYR, blue line), and CDs3 in the presence of a mixture containing 20 $\mu\text{g mL}^{-1}$  TYR and 0.32 mM L-DOPA(CDs3-TYR- L-DOPA, green line), respectively.

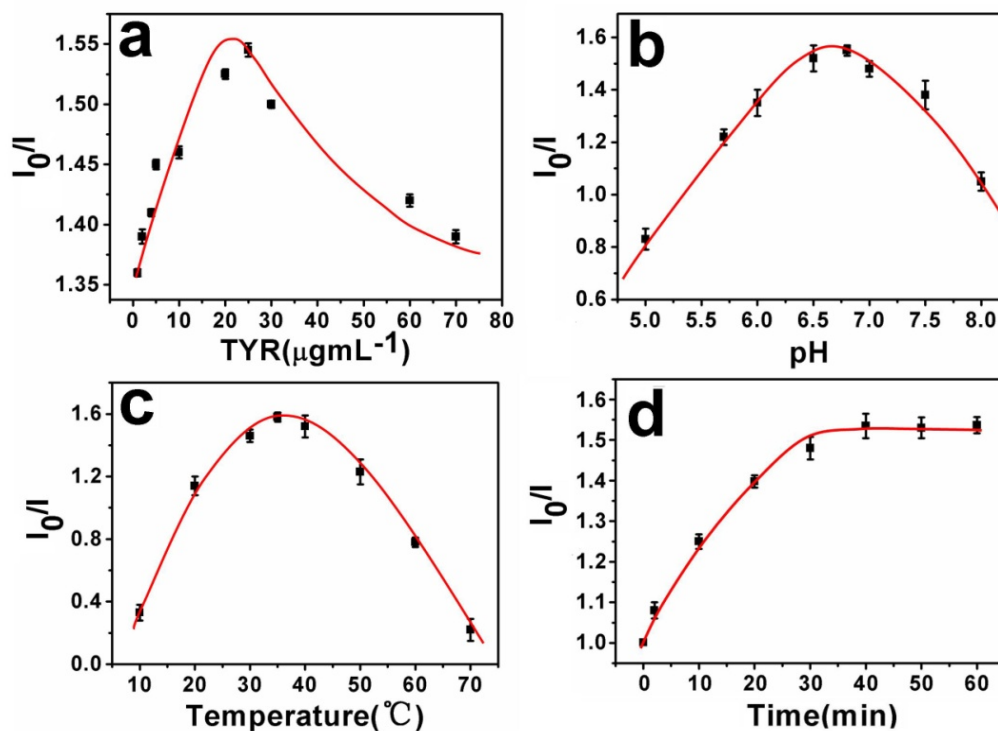


**Figure S11.** The effects of different TYR concentrations (a), pH (b), temperatures (c) and incubation times (d) on the quenched efficiency of the CDs1 in the presence of 0.13 mM L-DOPA and 20 $\mu\text{g mL}^{-1}$  TYR( $I_0$  and  $I$  are CDsPL intensity in the absence and presence of analysts, respectively).

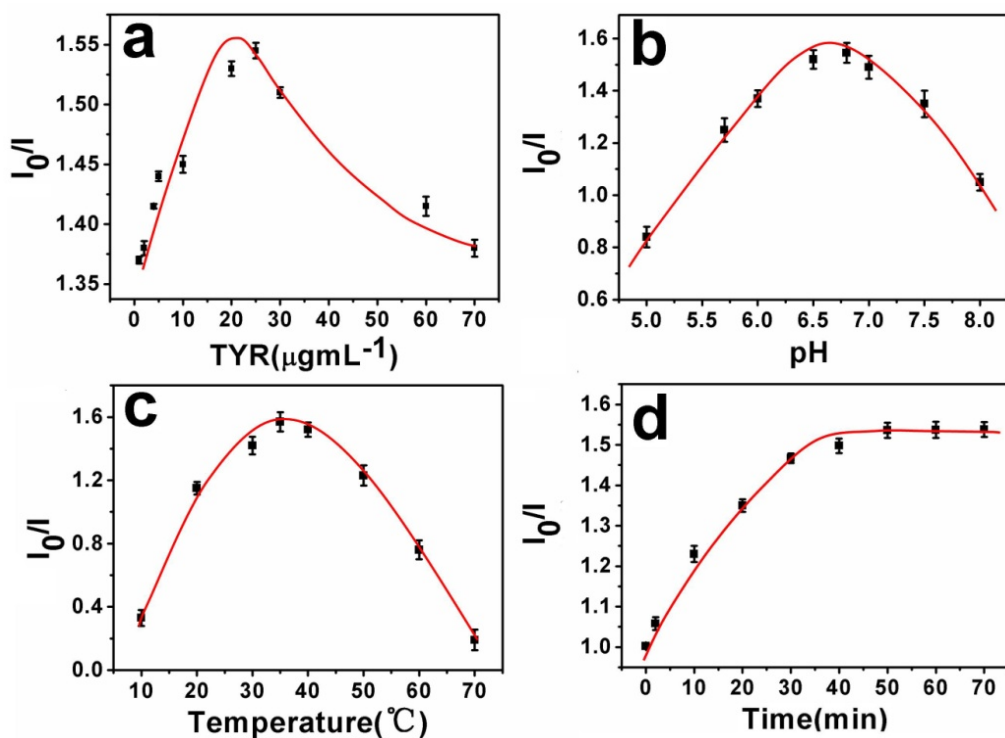


**Figure S12.** The effects of different TYR concentrations (a), pH (b), temperatures (c) and incubation times (d) on the quenched efficiency of the CDs3 in the presence of 0.13 mM L-DOPA and  $20\mu\text{g mL}^{-1}$  TYR ( $I_0$  and  $I$  are CDsPL intensity in the absence and presence of analytes, respectively).

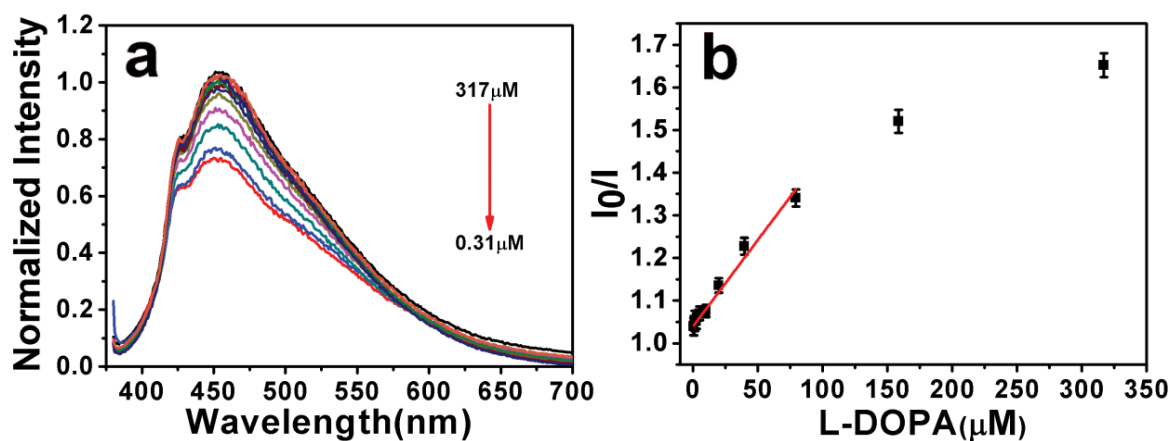


**Figure S13.** (a) The normalized fluorescence spectra of CDs1 containing  $20\mu\text{g mL}^{-1}$  TYR upon addition of different concentrations of L-DOPA from 317  $\mu\text{M}$  to 0.31  $\mu\text{M}$ . (b) The linear response of the quenching efficiency  $I_0/I$  of the CDs1 vs. concentrations of L-DOPA.

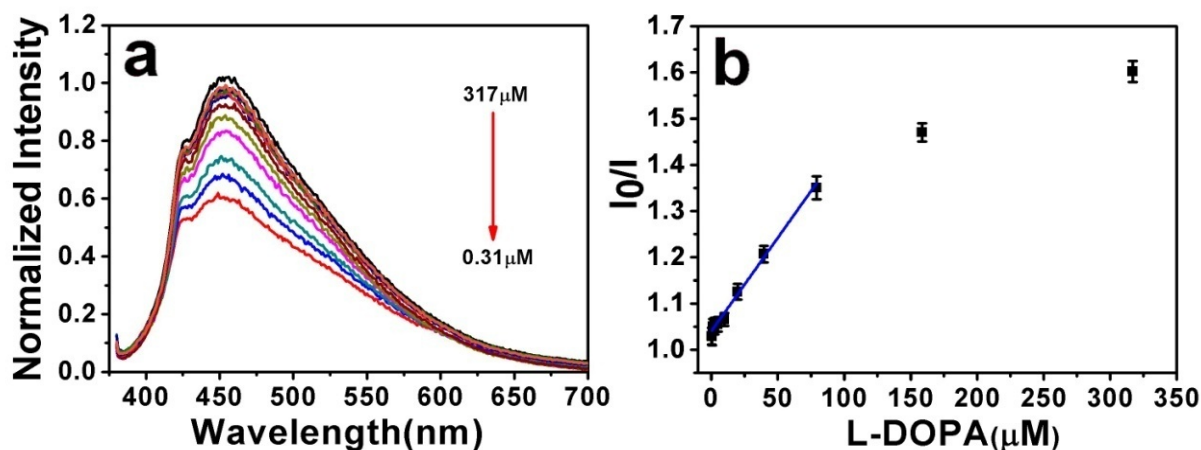


**Figure S14.** (a) The normalized fluorescence spectra of CDs3 containing  $20 \mu\text{g mL}^{-1}$  TYR upon addition of different concentrations of L-DOPA from  $317 \mu\text{M}$  to  $0.31 \mu\text{M}$ . (b) The linear response of the quenching efficiency  $I_0/I$  of the CDs3 vs. concentrations of L-DOPA.

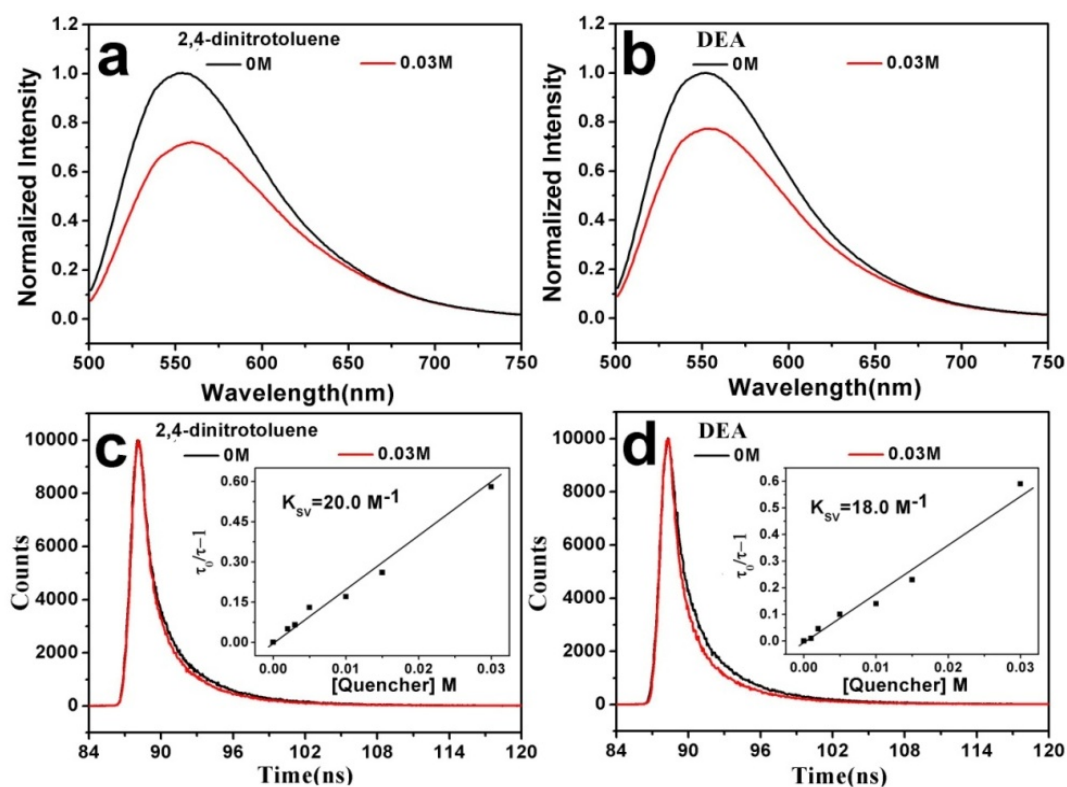


**Figure S15.** (a and b) Luminescence quenching spectra (485 nm excitation) of the CDs1 in toluene without and with the quencher (2,4-dinitrotoluene and DEA, both 0.03 M). (c and d) Luminescence decays (485 nm excitation, monitored with 550 nm narrow bandpass filter) of the CDs1 with 2,4-dinitrotoluene and DEA, respectively. Inset: Stern-Volmer plots for the quenching of luminescence quantum yields (485 nm excitation) of the CDs1 by (c) 2,4-dinitrotoluene and (d) DEA.

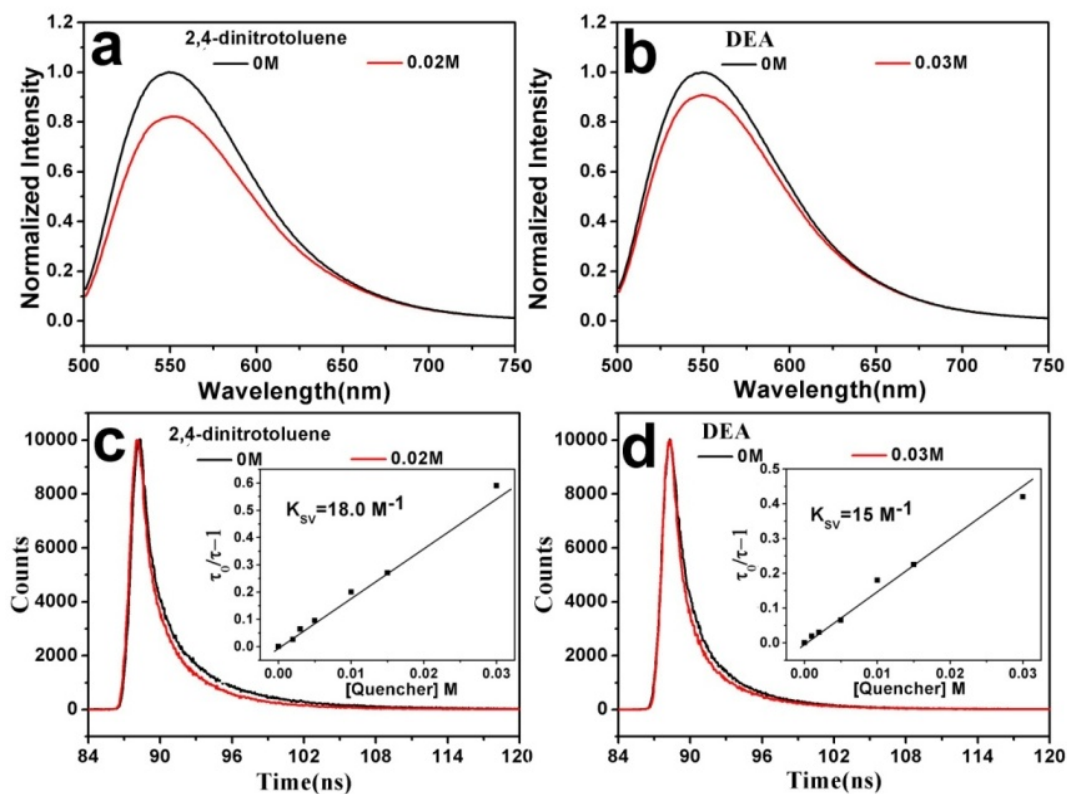


**Figure S16.** (a and b) Luminescence quenching spectra (485 nm excitation) of the CDs3 in toluene without and with the quenchers (2,4-dinitrotoluene and DEA, both 0.03 M). (c and d) Luminescence decays (485 nm excitation, monitored with 550 nm narrow bandpass filter) of the CDs3 with 2,4-dinitrotoluene and DEA, respectively. Inset: Stern–Volmer plots for the quenching of luminescence quantum yields (485 nm excitation) of the CDs3 by (c) 2,4-dinitrotoluene and (d) DEA.



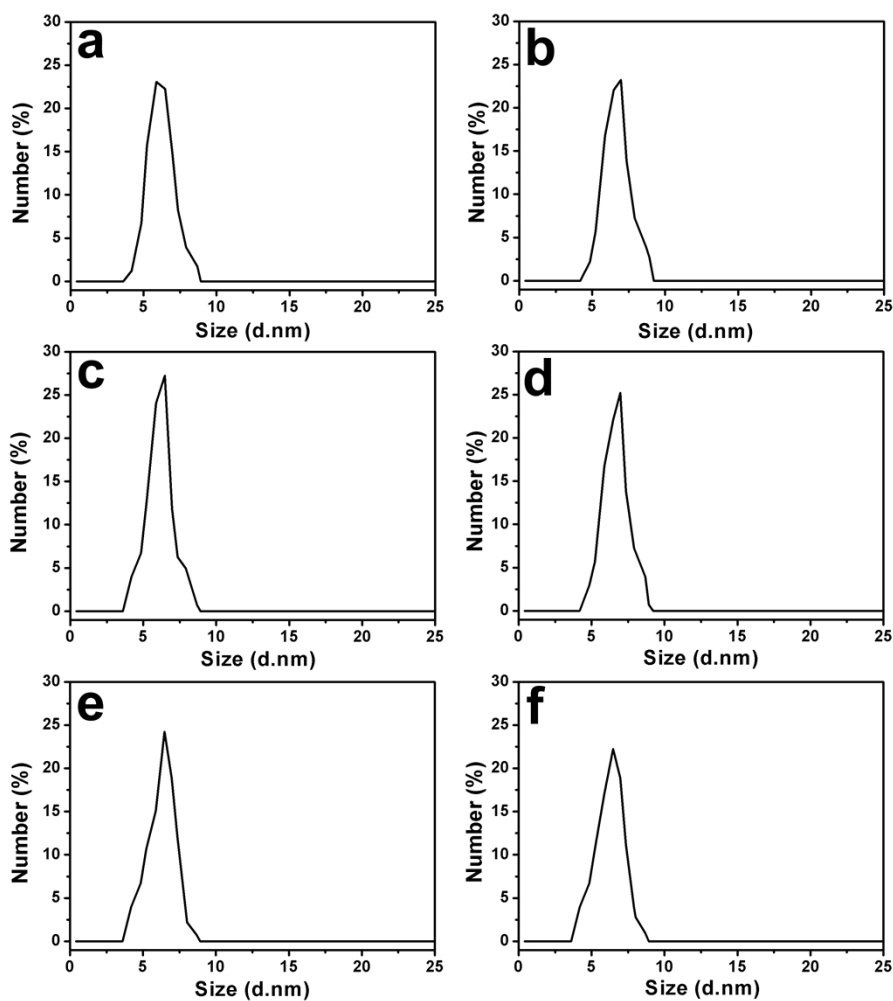


**Figure S17.** The DLS of CDs. (a) CDs1. (b) CDs2. (c) CDs3. (d) CDs4. (e) CDs5. (f) CDs6.

**Table S1.** Determination of L-DOPA in human blood sample using HPLC (clinical detection) and fluorescence detection method (RE: Test paper detection vs. HPLC clinical detection. RE<sub>1</sub>: CDs1, RE<sub>2</sub>: CDs2, RE<sub>3</sub>: CDs3).

Sample	HPLC ( $\mu\text{M}$ )	Fluorescence detection( $\mu\text{M}$ )			Relative error (%)		
		CDs1	CDs2	CDs3	RE <sub>1</sub>	RE <sub>2</sub>	RE <sub>3</sub>
1	156	145 $\pm$ 6	150 $\pm$ 4	149 $\pm$ 9	-7.05	-3.85	-4.49
2	95	90 $\pm$ 7	100 $\pm$ 5	102 $\pm$ 8	-5.26	+5.27	+7.37
3	82	82 $\pm$ 8	80 $\pm$ 3	90 $\pm$ 6	0	-2.45	+9.75
4	55	50 $\pm$ 9	60 $\pm$ 5	50 $\pm$ 8	-9.09	+9.09	-9.09
5	20	25 $\pm$ 8	20 $\pm$ 3	15 $\pm$ 5	+25	0	-25
6	4.5	5 $\pm$ 1.5	5 $\pm$ 1	2 $\pm$ 3	+11.11	+11.11	-66.67